Millimeter-Wave Monolithic Integrated Circuit Characterization by a Picosecond Optoelectronic Technique

HING-LOI A. HUNG, SENIOR MEMBER, IEEE, PENNY POLAK-DINGELS, MEMBER, IEEE, KEVIN J. WEBB, MEMBER, IEEE, THANE SMITH, SENIOR MEMBER, IEEE, HO C. HUANG, SENIOR MEMBER, IEEE, AND CHI H. LEE, SENIOR MEMBER, IEEE

Abstract—**The characterization of microwave and millimeter-wave monolithic integrated circuits (MIMIC's) using picosecond pulse sampling techniques is developed, with emphasis on improving broad-band coverage and measurement accuracy. GaAs photoconductive switches are used for signal generation and sampling operations. The measured time-domain response allows the spectral transfer function of the MIMIC to be obtained. This measurement technique was verified by characterization of the frequency response (magnitude and phase) of a reference 50 Ω microstrip line and a two-stage K_a-band MIMIC amplifier. The measured broad-band results agree well with those obtained from conventional frequency-domain measurements using a network analyzer. The application of this optical technique to on-wafer MIMIC characterization is also described.**

I. Introduction

GALLIUM ARSENIDE (GaAs) microwave and millimeter-wave devices and monolithic integrated circuits are currently being developed for applications such as satellite communications, radar, and phased-array systems. The conventional frequency-domain approach for testing these discrete devices and microwave and millimeter-wave monolithic integrated circuit (MIMIC) chips usually constitutes one of the major costs of a development program. This is especially true for devices and circuits operating in the millimeter-wave regime. Therefore, a low-cost testing technique which allows on-wafer characterization of MIMIC's before dicing the wafer into individual chips is highly desirable.

In addition to the cost factor, the evaluation of these devices becomes more difficult as applications extend to the higher millimeter-wave frequencies. Fairly accurate characterization of active devices and monolithic circuits can be achieved by using a waveguide measurement system that offers small attenuation, and with careful design may achieve low mismatch loss. However, this approach is inherently limited by the waveguide bandwidth, resulting in the need for multiple calibrations for different waveguides when measurements are made over a wide frequency range. Furthermore, high-performance waveguide-to-microstrip transitions for each waveguide band, as well as careful assembly of the interface between these transitions and the MIMIC test block, are required. Such an evaluation process is quite time consuming. In addition, oscillation may occur during the characterization of active devices that are not terminated with matching circuits. This problem occurs because of the purely reactive termination presented by the waveguide below its fundamental-mode cutoff frequency.

Current commercially available on-chip characterization systems for MIMIC's have provided useful performance data in the lower microwave range, and attempts are being made to extend their frequency of operation. However, several fundamental limitations still exist. Because these systems use special coplanar waveguide (CPW) probes [1], it is difficult to achieve a low-loss, impedance-matched probe at millimeter-wave frequencies. The operating life of such a mechanical direct-contact probe is usually quite limited, and a customized probe card is required for each set of microwave circuits on the wafer. The circuits also require CPW patterns to be incorporated at various test locations on the wafer.

Recently, optical techniques have been used in the characterization of microwave devices and circuits. Frequency-domain measurements have been performed using electro-optic probing of a microstrip line [2], [3]. In this work, the microwave signal was launched onto the circuit using CPW contacting probes. Valdmanis and Mourou [4] have demonstrated that, by using an electro-optic probe containing polar material such as lithium tantalate, substrates which do not exhibit the electro-optic effect can still be probed. Some results for a discrete GaAs field-effect transistor (FET) mounted on a silicon-on-sapphire (SOS) test circuit have been presented by Cooper and Moss [5]. In their work, a pulse generation/sampling technique using SOS photoconductors to obtain frequency-domain scattering parameters for the FET was demonstrated,

Manuscript received September 9, 1988; revised February 27, 1989. Part of this material was presented at the 1988 IEEE MTT-S International Microwave Symposium (New York, NY).

H-L. A. Hung, T. Smith, and H. C. Huang are with COMSAT Laboratories, Clarksburg, MD 20871-9475.

P. Polak-Dingels is with the University Research Foundation, Greenbelt, MD 20770.

K. J. Webb and C. H. Lee are with the Department of Electrical Engineering, University of Maryland, College Park, MD 20742.

IEEE Log Number 8928326.

0018-9480/89/0800-1223$01.00 ©1989 IEEE

and the results were compared with the manufacturer's data. This approach has been extended for on-wafer implementation of monolithic circuits using GaAs photoconductive switches, including an experimental study of its accuracy and sensitivity [6], [7].

This paper describes an optoelectronic technique employing a picosecond pulse source which can be used for on-wafer MIMIC characterization. The approach does not require high-frequency mechanical contact between the measuring system and the wafer for either waveform generation or sampling at millimeter-wave frequencies. The same measuring system allows broad-band operation from dc to 100 GHz, and can be extended to higher frequencies, depending on the optical pulse rise and fall times and the photoconductive switch dynamics. A proof-of-concept model of the optoelectronic technique was successfully demonstrated on a K_a-band (28 GHz) monolithic power amplifier circuit. Emphasis was placed on a systematic study of the validity of this time-domain measurement technique compared to the conventional frequency-domain measurement approach. For the same MIMIC, good agreement was found in a direct comparison of the magnitude and phase of the frequency response obtained using the optoelectronic technique with those from a conventional network analyzer measurement.

The sampling technique and two-port analysis are presented in Section II. The optical measurement system is described in Section III, and the measured results are presented in Section IV. Section V describes the implementation of the optoelectronic technique for on-wafer testing and compares this approach with other optical techniques. Section VI summarizes the significant results.

II. Analysis

The proposed technique was adapted from a picosecond photoconductivity measurement technique developed by Auston [8], [9]. This technique assumes a sufficiently low optical intensity such that small-signal conditions apply. Fig. 1 illustrates the generation and sampling operations. The time-dependent portion of the sampled signal as a function of delay time has been shown to correspond to a cross-correlation between the electrical signal on the line and the photconductive response of the sampling gap. The generation and sampling time responses are determined by the photoconductance of the gaps, which also include the contribution of the laser pulse width. For identical generation and sampling photoconductors, the time-dependent sampled signal, $g_{xy}(t)$, is the cross-correlation of the voltage pulse on the line at the output, $y(t)$, and the generated voltage, $x(t)$, as

$$g_{xy}(t) = \int_{-\infty}^{\infty} x(\tau)\, y(t+\tau)\, d\tau. \tag{1}$$

Fig. 2 is a schematic diagram of the optoelectronic characterization system, including the device under test (DUT). A short electrical pulse is generated by a dc-biased photoconductive switch [10] at port a and travels down the input transmission line toward the DUT. The pulse

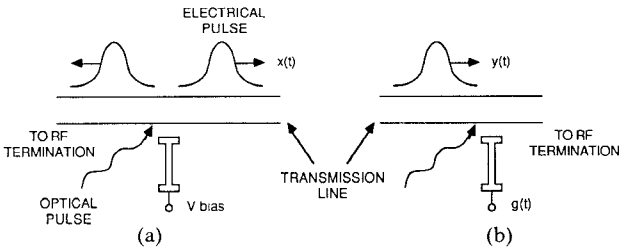

Fig. 1 Schematic of electrical pulse generation and sampling. (a) Generation. (b) Sampling.

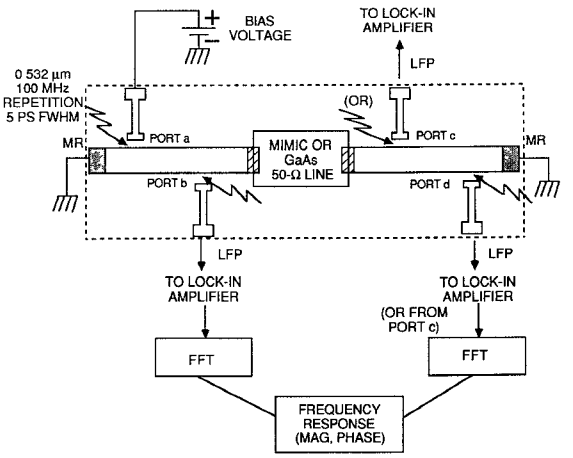

MR MONOLITHIC RESISTOR OR MATCHED LOAD
LFP LOW-FREQUENCY PROBE

Fig 2. Schematic of the two-port S-parameter measurement system.

traveling in the opposite direction is absorbed by the matched termination, which at present is coaxial load but which can readily be implemented as an integrated monolithic resistor (MR). The pulse approximates a delta function in the time domain, resulting in a very broad frequency spectrum. Since the input electrical pulse generated is in complete time synchronization with the optical pulse, this electrical pulse can be precisely sampled at port b by a time-delayed laser pulse illuminating a second picosecond photoconductive switch on the input side of the DUT.

The output of the DUT can be sampled using the same procedure, with a photoconductive switch at the output of the device (port c or d). By comparing the Fourier transforms of the transmitted and reflected waveforms to those of the incident waveform, the two-port scattering parameters can be determined without using CPW probes.

In the following analysis (referenced to the measurement system schematic shown in Fig. 2), a picosecond electrical pulse is generated at port a. The signal at port b corresponds to an autocorrelation of the voltage pulse, $f_t(t)$, created at port a (assuming identical photoconductors at ports a and b) and is obtained by illumination of the gaps associated with ports a and b. The time-dependent sampled signal at port b is given by

$$g_{bi}(t) = f_t(-t) * f_t(t) \tag{2}$$

where $*$ represents the convolution operation, the first subscript on $g(t)$ refers to the port identification, and the

second refers to the incident (i), reflected (r), or transmitted (t) signal, depending on which is measured. In (2) it is assumed that the time-domain signal is windowed (by selecting the length of sampling time) so that only the contribution from the incident signal is measured. The frequency-domain spectrum of the sampled input signal at port b is

$$G_{bi}(f) = |F_i(f)|^2. \tag{3}$$

If the time-domain window at port b is such that only the reflected signal $f_r(t)$ is sampled, then the reflected time-domain waveform

$$g_{br}(t) = f_i(-t) * f_r(t) \tag{4}$$

can be obtained. Thus, the spectrum of the windowed reflected signal which is sampled is

$$G_{br}(f) = F_i^*(f) \cdot F_r(f) \tag{5}$$

where F_i^* is the complex conjugate of F_i.

At the output of the MIMIC, the voltage pulse is given by

$$f_o(t) = h(t) * f_i(t) \tag{6}$$

where $h(t)$ is the impulse response of the DUT. The photoconductive switches in the output network are the same as those used for generation and sampling in the input network. The sampled signal at port c or d is given by the cross-correlation of $f_i(t)$ with $f_o(t)$, or

$$g_{ct}(t) = f_i(-t) * f_o(t). \tag{7}$$

The Fourier transform of $g_{ct}(t)$ is therefore

$$G_{ct}(f) = |F_i(f)|^2 H(f). \tag{8}$$

The complex input scattering parameters, $S_{21}(f)$ and $S_{11}(f)$, for the DUT can thus be expressed as a function of frequency as

$$S_{21}(f) = \frac{G_{ct}(f)}{G_{bi}(f)} \tag{9}$$

$$S_{11}(f) = \frac{G_{br}(f)}{G_{bi}(f)}. \tag{10}$$

Equations (9) and (10) establish the phase reference planes at ports b and c; however, these references can be adjusted. The complex scattering parameters, $S_{12}(f)$ and $S_{22}(f)$, can also be obtained in a similar manner. The time-domain to frequency-domain transforms are performed numerically using the fast Fourier transform (FFT) algorithm on a Hewlett-Packard (HP) minicomputer, which was also used to control the experiment.

III. Measurement System

The optical system and components, including the laser source and the GaAs photoconductive switch to generate the electrical pulse, are now described.

A. The Optical Source

The optical system is shown schematically in Fig. 3. It consists of a continuous-wave, actively mode-locked Nd:YAG laser, whose output is compressed by a fiber-grating pair pulse compressor and then frequency-doubled by passing through a potassium titanyl phosphate (KTP) crystal. The optical pulses have a wavelength of 532 nm (green spectrum), a repetition rate of 100 MHz, a full-width-at-half-maximum (FWHM) pulse duration of 5 ps, and an average power of 400 mW. The laser output is split into two beams: one focused on the pulse generator photoconductive switch, and the other on the sampling gate, with a typical fluence of 30 μJ/cm^2. Two separate stepper motors vary the length of the delay line between the two laser beams: a high-resolution stage with a step size of 0.4 μm and a total travel distance of 5 cm, and a longer delay stage with a step size of 10 μm and a total travel length of 15 cm. Thus, the optical delay line can provide a variable time delay of 1.3 ns between the two beams, with a resolution of 0.01 ps. The pulse train illuminating the generator gap was chopped at 200 Hz, and the resultant signal from the sampling gap was fed to a lock-in amplifier.

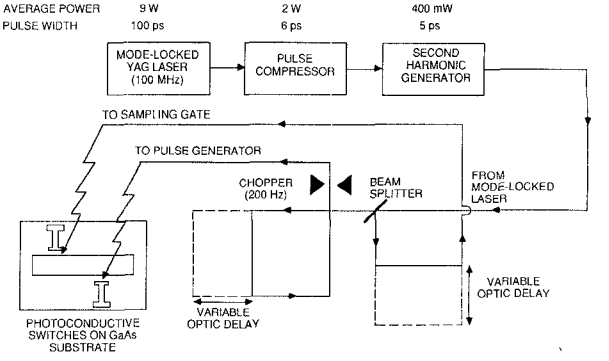

Fig. 3. Optical system with delay line and switch.

B. Photoconductive Switch

The optically activated photoconductive switches for picosecond pulse generation consist of 100-μm-wide by 5-μm-long gaps between metal conductors on a 245-μm-thick liquid-encapsulated Czochralski (LEC) grown GaAs semi-insulating substrate. They were fabricated between a planar 50 Ω microstrip line and a shunt high-impedance line. The gaps were proton-implanted at 150 keV with hydrogen at a dose of 10^{14}/cm^2 on the surface of the substrate, in order to reduce the carrier lifetime. Oxygen implantation at a lower dosage can also be used. A Ti–Au metal conductor thickness of 3 μm was used to achieve sufficiently low conductor loss. The shunt microstrip lines were designed to minimize the discontinuity seen by the electrical pulse in the optical measurement, and by the microwave signal used in the experimental validation tests with the network analyzer, propagating along the 50 Ω transmission line. Measurements on a switch circuit and a GaAs 50 Ω line of the same physical length confirmed that the presence of the switches did not affect the transmission characteristics of the pulses or the microwave signals. In addition, a reference measurement with respect to a 50 Ω microstrip line (the same length as the MIMIC) was performed prior to the actual measurement, and the calibra-

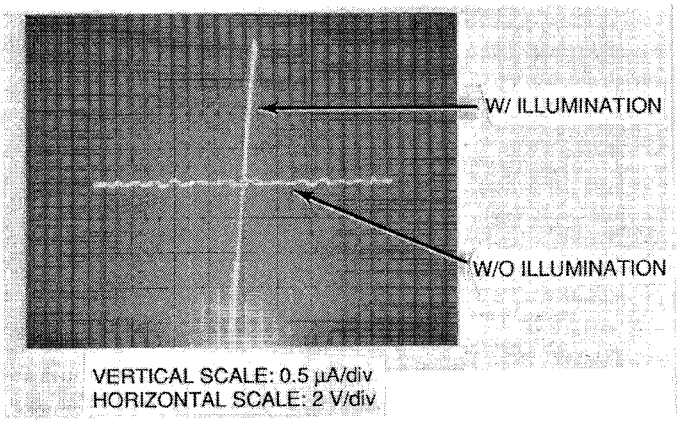

Fig. 4. dc characterization of the optical switch.

tion data were used to normalize the magnitude and the phase for the MIMIC.

When photons are absorbed in GaAs, electron–hole pairs are created, increasing the conductivity of the illuminated GaAs. In a biased photoconductor, the photoconductive signal responds instantaneously to the optical pulse. The decay of the photoconductive signal is influenced by carrier recombination and carrier sweep-out. The process with the shorter characteristic time constant dominates the photoconductive signal decay process.

In very pure GaAs, the recombination time is measured in microseconds [11], a factor of approximately 10^6 longer than the required pulse length. Carriers in GaAs have a saturation velocity of approximately 0.1 μm/ps. If a constant electric field greater than 0.3 V/μm can be maintained across the gap, the carrier sweep-out time for a 5 μm gap is 50 ps. However, in undamaged semi-insulating GaAs, current is observed to persist for as much as 200 ps after illumination of the gap ceases. This is because the electric field in the gap "collapses," creating a low field region in the center of the gap from which carriers leak relatively slowly.

The solution to the above problem is to heavily damage the GaAs lattice in the gap by proton implantation. This creates a high density of recombination centers, which reduces the recombination time to the subpicosecond range in SOS [12] and, in the present work, to approximately 10 ps in GaAs. The trade-off for this is an increase in the illuminated resistance by a factor of 2 or more and a decrease in the dark resistance due to conduction via defect sites. The photoconductive switches for the present study typically have a dark resistance of several megohms, and with sufficiently intense illumination can have an illuminated resistance as low as several ohms. Fig. 4 shows the change in conductance as indicated in the I–V characteristics of a switch with illumination from a microscope light source and without illumination.

The measured FWHM pulse length at port b is 10 to 12 ps, close to the resistance/capacitance (RC) time constant of the photoconductive gap [13]. Therefore, to obtain shorter pulses, it is necessary to reduce this time constant. When the time constant becomes negligible, the pulse length becomes the sum of the optical pulse length (5 ps in the present case) and the carrier recombination time. The carrier recombination time can be reduced, if necessary, by increasing the proton bombardment fluence. Shorter optical pulses will also decrease the electrical pulse duration. Optical pulses from lasers with a duration of 80 fs [14], [15] have been used to make optical sampling measurements.

IV. Experimental and Numerical Results

Measured results were obtained for both a 50 Ω line reference circuit and an MIMIC using the optical and network analyzer techniques. This section presents a comparison of these results.

A. Test Circuits

Two GaAs circuits were tested: the reference and the MIMIC to be characterized. The reference circuit consisted of a sample 50 Ω microstrip line for overall system calibration. The MIMIC to be tested was a two-stage power amplifier with a nominal gain of 4 dB per stage and an output power close to 0.5 W at 28 GHz [16]. Fig. 5 shows the nominal performance of a one-stage MIMIC measured in a waveguide housing. An output power of 1 W was achieved with these MIMIC's in a balanced configuration.

The MIMIC tested was mounted between two circuits, each containing two photoconductive switches. Fig. 6 is a photograph of the switch/MIMIC assembly. In the implementation of this technique, the bias of the switch and the collection of the signal are achieved with simple low-frequency probes (LFP's) at the end of the high-impedance shunt transmission lines. Since the sampled signals are at the 200 Hz chopper frequency, coaxial LFP's such as those used in the existing automated on-wafer dc characterization are needed to pick up the sampled signal, eliminating the need for expensive microwave CPW probes. In the experiment, a bias voltage of 20 V was applied to the photoconductive switches. This produces a voltage pulse amplitude of 80 mV, which is well within the linear range of the MIMIC amplifier.

B. Measured Results

The measured autocorrelation signal at port b is shown in Fig. 7 for the case where data have been taken every 0.5 ps. A similar time response was obtained at the output port when the reference circuit was tested. In order to correctly determine the phase response of the device, the time delay between the signal at the input port and the signal at the output port was determined by moving the delay stage. For the reference circuit, this delay was 186 ps. The time-domain data obtained at the output were shifted by this delay time before the FFT was performed. Fig. 8 shows the transfer function magnitude and phase response of the 50 Ω reference line after the FFT of the time domain data. A 4000 point FFT was used to obtain each set of the input and output spectral-domain data; the measured data were padded with zeros.

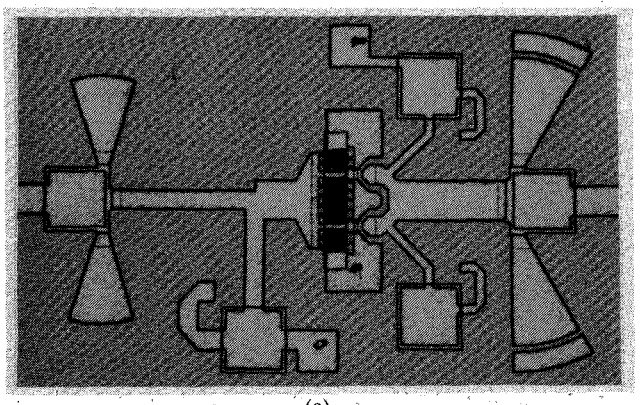

(a)

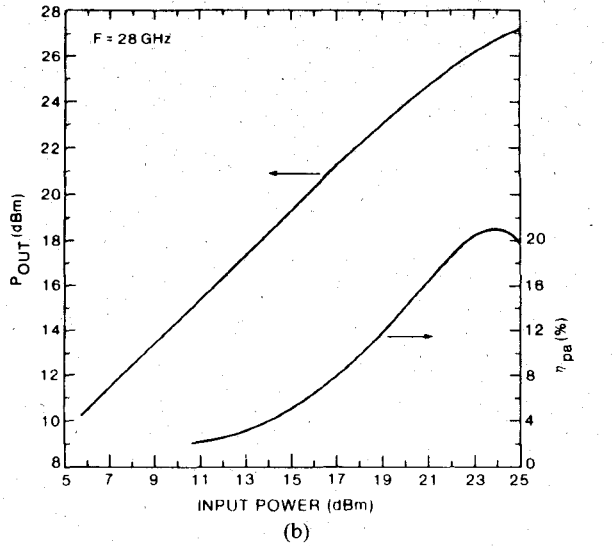

(b)

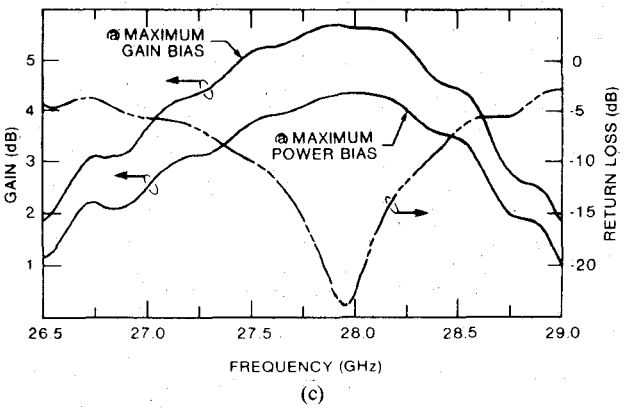

(c)

Fig. 5. K_a-band MIMIC and performance of a single-stage amplifier. (a) K_a-band MMIC. (b) P_{out} and η_{pa} versus input power. (c) Gain response.

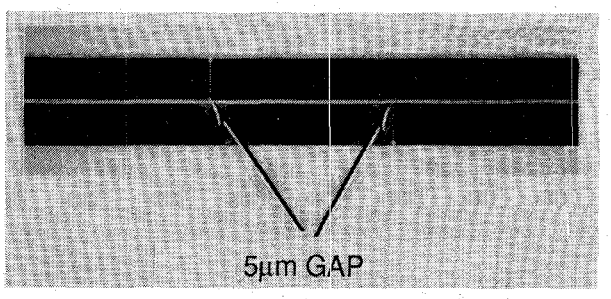

(a)

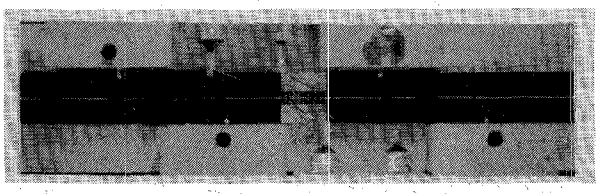

(b)

Fig. 6. (a) GaAs optoelectronic switch and (b) MIMIC/switch assembly.

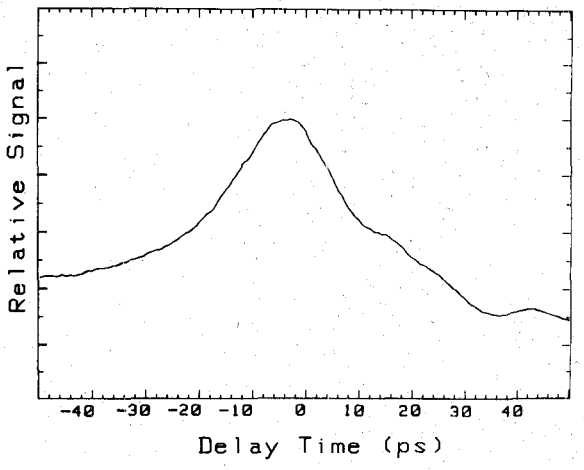

Fig. 7. Time-domain correlation response measured at the input of the reference line (including dc leakage of the bias voltage).

To verify these measured results, the transfer function of the 50 Ω reference circuit was measured using an HP8510 network analyzer. An additional reference test fixture was also measured to eliminate the effect of the coaxial launchers used in the reference line and in the MIMIC measurements in the frequency domain. The reference circuit contained an appropriate length of GaAs 50 Ω microstrip line for circuit loss calibration. The transfer function for the reference line determined by this method is depicted in Fig. 9. The good agreement between the results in magnitude and phase, as shown in Figs. 8 and 9, confirms the accuracy of the optoelectronic technique.

For the MIMIC circuit, the time-domain signal obtained at the input port is similar to that of Fig. 7. The electrical pulse waveform detected at the output, which is shown in Fig. 10, consists of 800 points taken at 0.5 ps intervals. Since the electrical pulse was amplified through the MIMIC with a narrow bandwidth around 28 GHz, the pulse at the output is expected to have a much broader waveform compared to that at the input.

The magnitude and the phase of the transfer function, S_{21}, as determined by the FFT program of the data obtained from the optical technique are shown in Fig. 11. This figure can be compared with Fig. 12, which shows the transfer function measured by the network analyzer tech-

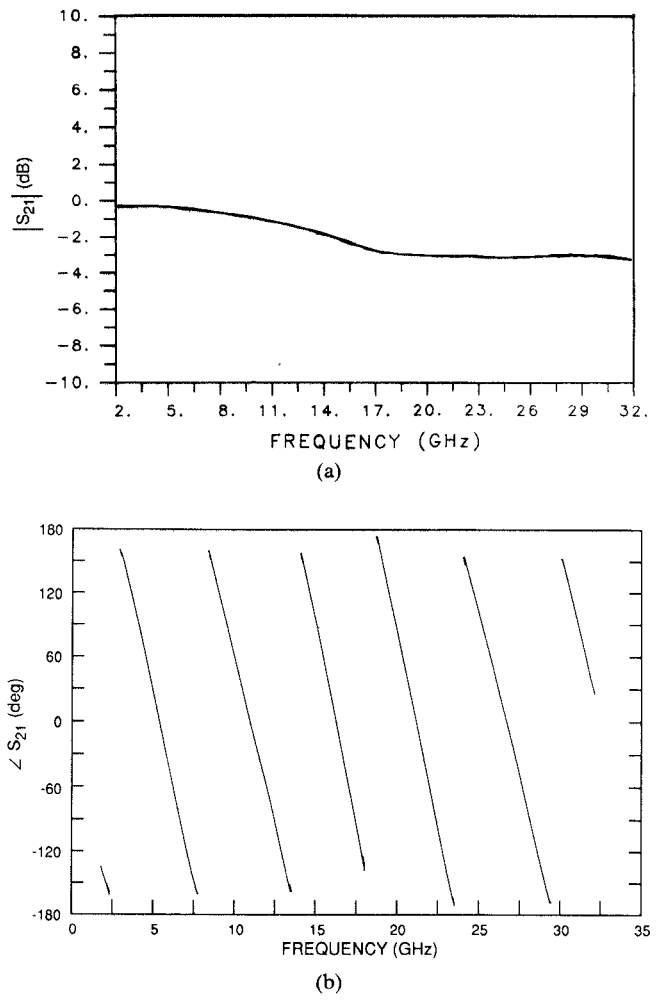

Fig. 8. Frequency response of 50 Ω reference line from optoelectronic technique. (a) Magnitude. (b) Phase.

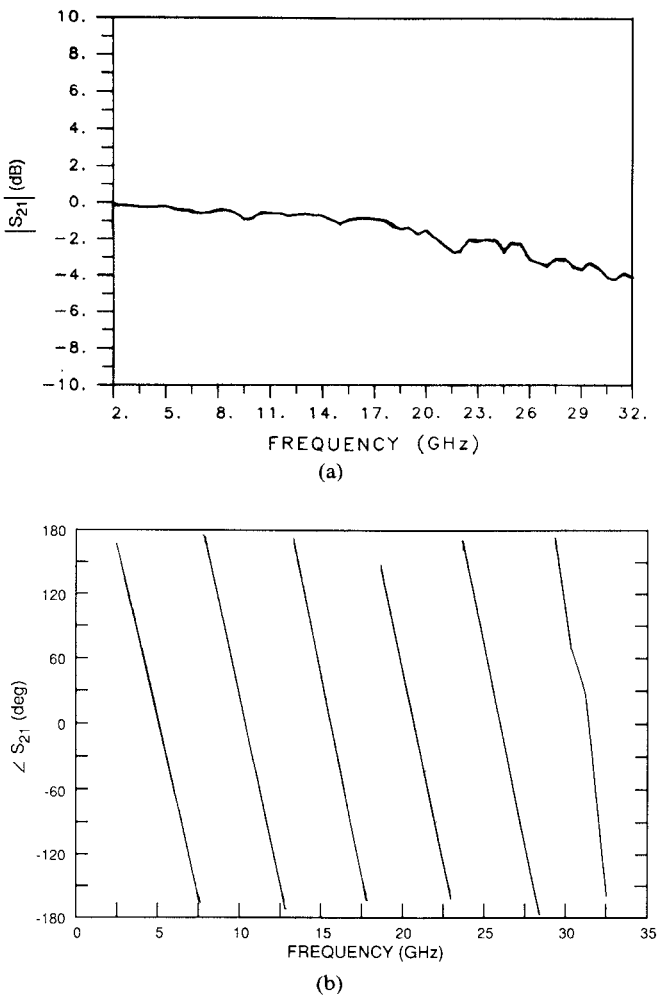

Fig. 9. Frequency response of 50 Ω reference line from network analyzer measurement. (a) Magnitude. (b) Phase.

nique. Good agreement in the broad-band response was obtained. S_{11} can be determined in a similar manner. In this case, both the input and the reflected pulses are measured at the input port. This measurement is being studied with an emphasis on the dynamic range [17].

The optoelectronic technique has provided good results for S parameters when compared to frequency-domain network analyzer measurements. The dynamic range of the time-domain technique achieved thus far is less than that from the HP8510 network analyzer when comparison is made at the lower microwave frequency range. However, this dynamic range can be improved by limiting the bandwidth of the optically generated electrical pulse. If broad-band data are required, the time-domain technique produces these data in one measurement, rather than as a superposition of frequency-domain measurements. Therefore, there is a bandwidth/signal-to-noise trade-off.

The sensitivity of the present optoelectronic switch is also limited by the switch-off characteristics of the present photoconductors, which exhibited some leakage current. Better photoconductive switches can be fabricated to overcome this difficulty. The pulse amplitude could be raised by reducing the on-state resistance with a lower fluence of protons, increasing the photoconductive gap size, or using higher voltage across the switch.

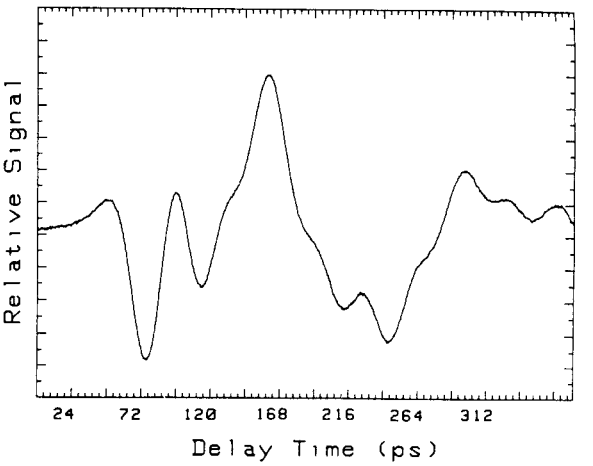

Fig 10. Time-domain response at the output of the K_a-band MIMIC.

V. On-Wafer Implementation

At present, auxiliary test structures on separate chips are used to implement the optoelectronic characterization technique. For application to on-wafer characterization,

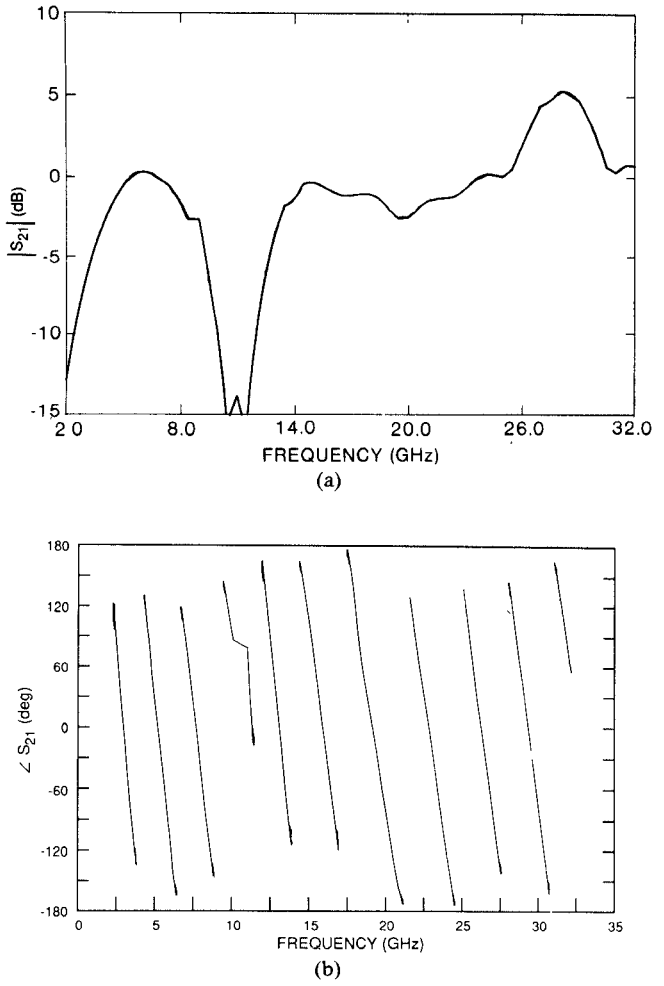

Fig. 11. Frequency response of K_a-band two-stage MIMIC amplifier from optoelectronic technique. (a) Magnitude. (b) Phase.

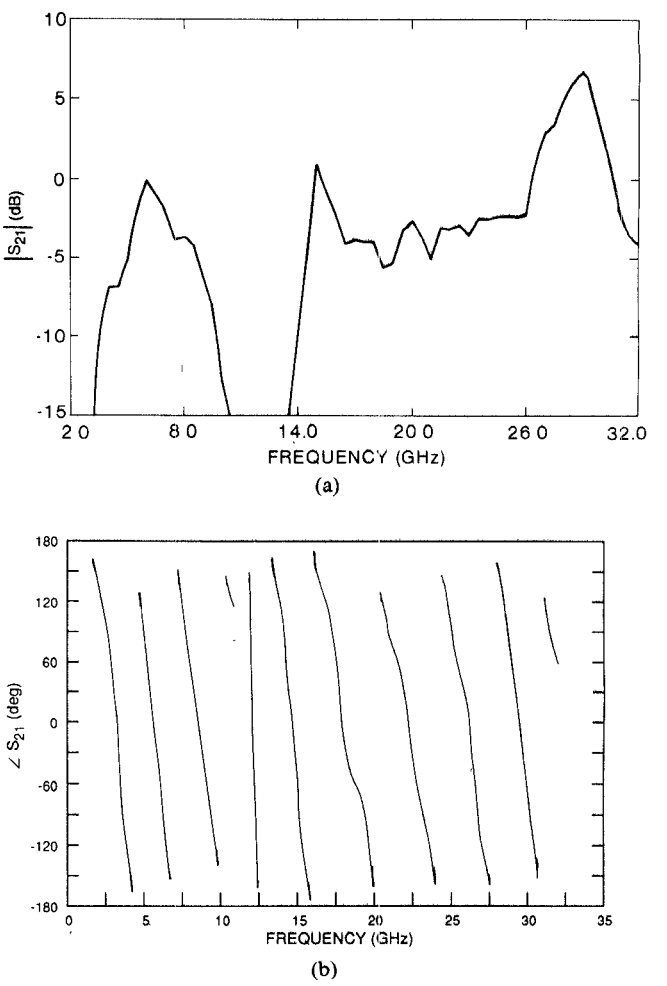

Fig. 12. Frequency response of K_a-band two-stage MIMIC amplifier from network analyzer measurement. (a) Magnitude. (b) Phase.

the mask set can be designed with microstrip test structures connected to the MIMIC's to be characterized. A pulse generation optical switch and a pulse sampling port (which can be an identical optical switch) must be placed at sites along the line. The line length limit is determined by the need to resolve incident from reflected signals and to remove spurious reflections. The line lengths can be shortened by using electrical signals of shorter duration or by performing additional measurements and enhancing the FFT algorithm to separate the different signal waveforms. If these lines are made short and implemented in areas normally not occupied by devices (such as in saw kerfs around the border on each MIMIC chip or in test pattern locations), the required test patterns can be incorporated on the wafer while maintaining the same chip density.

To allow the measurement of scattering parameters at each MIMIC port, transmission lines terminated in their characteristic impedance may not be required, as they are in a conventional frequency-domain measurement method. In the pulse technique, this requirement can be eliminated by using appropriate time-domain windowing to remove the reflected pulses from the sampled data. Data collection is simply terminated before the reflected signal arrives at the sampling point. However, good RF terminations, especially on the output transmission line, will permit a reduction in the size of the test structure.

By using the photoconductive switch for broad-band spectral signal generation, electro-optic sampling could be employed, instead of built-in optical sampling switches along a transmission line. This has the advantage that the electric field (which is proportional to the voltage) at any point on the line, or even at any internal node within the MIMIC itself, can be selected for sampling [3], [4]. In addition, this sampling technique causes minimal discontinuity since no physical sampling structure is required. Also of interest is the fact that electro-optic sampling usually has better time resolution. In the present system, three factors contribute to the resolution limit: 2 ps due to optical transit time across the 100-μm-thick substrate, 60 fs due to the transit time of the electrical pulse across the 5 μm sampling spot, and 5 ps due to laser pulse duration. By using a laser pulse with shorter duration (0.1 ps is possible) and a thinner substrate, the time resolution may be improved to 1 ps [2]–[4].

The disadvantages of electro-optic sampling are that adequate electric field magnitude and exact placement of the optical signal are required in order to obtain a meaningful detected signal, and this approach works best with

materials that exhibit the electro-optic effect (such as GaAs). For measurements on materials which are not electro-optic, such as silicon, an electro-optic probe can be used [4]. In this case, the magnitude of the electric field is more critical, but the probe material could be chosen to have the largest possible electro-optic effect.

The electro-optic sampling approach is currently being applied to the testing of the same MIMIC used in the optoelectronic experiment. Preliminary test results indicate that similar time-domain waveforms have been obtained from both the photoconductive and electro-optic techniques [17].

VI. Conclusions

An optoelectronic characterization technique has been demonstrated to achieve broad-band frequency response for both the magnitude and the phase of a K_a-band MIMIC. The optical system has been calibrated using a reference measurement, and the measured scattering parameters show close agreement with data obtained from network analyzer measurements on the MIMIC amplifier. This technique offers significant potential for on-wafer characterization of both high-speed devices and high-frequency circuits.

Based on these experiments, an automated measurement system suitable for the manufacturing environment can be developed to achieve high throughput in on-wafer MIMIC evaluation. With an appropriate pulse width, the measurement system can be extended to frequencies above 100 GHz. Signal-to-noise ratio and dynamic range issues, as well as the application of the optical technique to measurement of the nonlinear and multiport characteristics of MIMIC components and subsystems, are currently being studied.

Acknowledgment

The authors would like to thank F. Phelleps, A. Meulenberg, D. Mullinix, T. Lee, and J. Chen of COMSAT Laboratories for their technical support.

References

[1] E. W. Strid, "26-GHz wafer probing for MMIC development and manufacture," *Microwave J.*, pp. 71–82, Aug. 1986.

[2] B. Kolner and D. Bloom, "Electro-optic sampling in GaAs integrated circuits," *IEEE J. Quantum Electron.*, vol. QE-22, pp. 79–93, Jan. 1986.

[3] K. J. Weingarten, M. J. W. Rodwell, and D. M. Bloom, "Picosecond optical sampling of GaAs integrated circuit," *IEEE J. Quantum Electron.*, vol. QE-24, pp. 198–220, Feb. 1988.

[4] J. A. Valdmanis and G. Mourou, "Subpicosecond electrical sampling and applications," in *Picosecond Optoelectronic Devices*, C. H. Lee, Ed. Orlando, FL: Academic Press, 1984, ch. 2, pp. 209–270.

[5] D. E. Cooper and S. C. Moss, "Picosecond optoelectronic measurement of the high-frequency scattering parameter of a GaAs FET," *IEEE J. Quantum Electron.*, vol. QE-22, pp. 94–100, Jan. 1986.

[6] H-L. A. Hung *et al.*, "Optical electronic characterization of monolithic millimeter-wave integrated circuits," in *12th Int. Conf. Infrared and Millimeter-Waves Dig.* (Orlando, FL), Dec. 1987, pp. 87–88.

[7] P. Polak-Dingels *et al.*, "On-wafer characterization of monolithic millimeter-wave integrated circuit by a picosecond optical electronic technique," in *IEEE MTT-S Int. Microwave Symp. Dig.* (New York, NY), May 1988, pp. 237–240.

[8] D. A. Auston, "Impulse response of photoconductor in transmission lines," *IEEE J. Quantum Electron.*, vol. QE-19, pp. 639–648, Apr. 1983.

[9] D. A. Auston, K. P. Cheung, J. A. Valdmanis, and P. R. Smith, "Ultrafast optical electronics: From femtoseconds to terahertz," in *Picosecond Electronics and Optoelectronics*, G. A. Mourou, D. M. Bloom, and C. H. Lee, Eds. Berlin: Springer-Verlag, 1985, pp. 2–7.

[10] C. H. Lee, Ed. *Picosecond Optoelectronic Devices*. Orlando, FL: Academic Press, 1984 (a general review of picosecond photoconductor optical sampling techniques).

[11] M. Neuberger, *III–V Semi-Conducting Compounds*, vol. 2 of *Handbook of Electronic Materials*. New York: IFI/Plenum, 1971, p. 48.

[12] F. E. Doany, D. Grischkowsky, and C-C. Chi, "Carrier lifetime versus ion-implantation in silicon on sapphire," *Appl. Phys. Lett.*, vol. 50, pp. 460–462, 1987.

[13] R. B. Hammond, N. G. Paulter, and R. S. Wagner, "Observed circuit limits to time-resolution in correlation measurements with silicon-on-sapphire, GaAs, and InP picosecond photoconductors," *Appl. Phys. Lett.*, vol. 45, pp. 289–291, 1984.

[14] D. Grischkowksy *et al.*, "Photoconductive generation of sub-picosecond electrical pulses and their measurement applications," in *Picosecond Electronics and Optoelectronics II*, F. J. Leonberger, C. H. Lee, F. Capasso, and H. Morkoc, Eds. Berlin: Springer-Verlag, 1985.

[15] M. B. Ketchen *et al.*, "Generation of sub-picosecond electrical pulses on coplanar transmission lines," *Appl. Phys. Lett.*, vol. 48, pp. 751–753, 1986.

[16] H-L. A. Hung *et al.*, "K_a-band monolithic power amplifiers," in *IEEE Microwave and Millimeter-Wave Monolithic Circuit Symp. Dig.* (Las Vegas, NV), June 1987, pp. 97–100.

[17] H-L. A. Hung *et al.*, "Characterization of GaAs monolithic circuits by optical techniques," in *SPIE Proc. Opt. Technol. for Microwave*, vol. 1102, July 1989.

✠

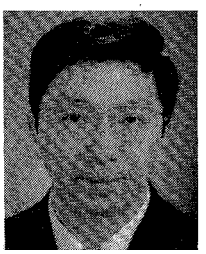

Hing-Loi A. Hung (S'67–M'75–SM'81) received the S.B.E.E. degree from the Massachusetts Institute of Technology, Cambridge, MA, in 1968 and the M.S. and Ph.D. degrees from Cornell University, Ithaca, NY, in 1970 and 1974, respectively.

He joined COMSAT Laboratories in 1974 and is currently Manager of the Monolithic Microwave Techniques Department. His present research areas include millimeter-wave monolithic integrated circuits and T/R modules, heterojunction devices, optoelectronics/microwave techniques, and MMIC reliability. He participated in satellite transponder designs for the INTELSAT V and VI, and COMSAT STC programs.

Dr. Hung has been a Professorial Lecturer at the George Washington University since 1978, and was Vice-Chairman and Chairman of the IEEE Electron Devices Society, Washington Section, from 1980 to 1982.

✠

Penny Polak-Dingels (M'88) received the B.S. degree in chemistry from the University of Illinois at Urbana. She then worked as an administrative assistant in the undergraduate chemistry program at the University of Illinois in Chicago. She returned to graduate school at that campus, completing the requirements for a Ph.D. in physical chemistry in 1979.

She has held postdoctoral appointments at the University of Maryland and the Naval Research Laboratory. Currently, she is a research scientist

at the University Research Foundation, Greenbelt, MD. Her research interests are in ultrafast phenomena and the kinetics of optoelectronic processes in semiconductor materials.

✠

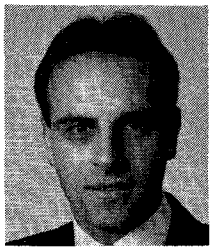

Kevin J. Webb (S'80–M'84) received the B.Eng. and M.Eng. degrees in communications and electronic engineering from the Royal Melbourne Institute of Technology, Australia, in 1978 and 1980, respectively; the M.S.E.E. degree from the University of California, Santa Barbara, in 1981; and the Ph.D. degree in electrical engineering from the University of Illinois, Urbana, in 1984.

Since 1984, he has been an Assistant Professor in the Electrical Engineering Department at the University of Maryland, College Park. His research interests include microwave and millimeter-wave integrated circuits, VLSI circuits, optoelectronics, numerical electromagnetics, and frequency selective surfaces.

Dr. Webb is a member of Tau Beta Pi, Eta Kappa Nu, and Phi Kappa Phi.

✠

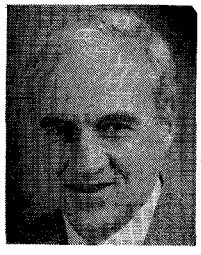

Thane Smith (M'73–SM'83) received the B.S. degree in physics from the Massachusetts Institute of Technology, Cambridge, MA, in 1962 and the M.S. and Ph.D. degrees from Carnegie Mellon University, Pittsburgh, PA, in 1964 and 1968, respectively.

He joined COMSAT Laboratories, Clarksburg, MD, in 1975, and is currently a Senior Scientist in the Microelectronics Division. His present research areas include picosecond optical switches in GaAs MMIC's, high-efficiency GaAs power FET's, monolithically compatible varactor diodes, GaAs MMIC VCO's, and the physics and modeling of FET's.

✠

Ho C. Huang (M'68–SM'80) received the B.S.E.E. degree from National Taiwan University in 1959 and the M.S. and Ph.D. degrees from Cornell University, Ithaca, NY, in 1965 and 1967, respectively.

He is currently Director of the Microelectronics Division at COMSAT Laboratories, Clarksburg, MD, where his responsibilities include research in III–V compound semiconductor materials, microwave device design, MIC and MMIC fabrication technology, and physical/chemical analysis. Prior to joining COMSAT in 1983, he was with RCA Laboratories.

Dr. Huang has served as Session Chairman for many IEEE technical conferences, and has been awarded seven U.S. patents. In 1983, he was granted the David Sarnoff Award for Outstanding Technical Achievement.

✠

Chi H. Lee (M'80–SM'86) received the B.S. degree in electrical engineering from National Taiwan University, Taipei, Taiwan, in 1959 and the M.S. and Ph.D. degrees in applied physics from Harvard University, Cambridge, MA, in 1962 and 1968, respectively.

He was with the IBM San Jose Research Laboratory from 1967 to 1968. Since 1968, he has been with the University of Maryland, College Park, where he is now a Professor of Electrical Engineering. His areas of research include picosecond optoelectronics, lasers, optical techniques for microwave application, and millimeter-wave devices.

Dr. Lee is a Fellow of the Optical Society for America and a member of the American Physical Society. He also serves as the Chairman of the IEEE MTT-3 Technical Committee for Lightwave Technology.